Remote measurements of X-rays dose rate using a cerium-doped air-clad optical fiber

Jessica Bahout, Youcef Ouerdane, Hicham El Hamzaoui, Géraud Bouwmans, Mohamed Bouazaoui, Andy Cassez, Karen Baudelle, Rémi Habert, Adriana Morana, Aziz Boukenter, et al.

▶ **To cite this version:**

Jessica Bahout, Youcef Ouerdane, Hicham El Hamzaoui, Géraud Bouwmans, Mohamed Bouazaoui, et al.. Remote measurements of X-rays dose rate using a cerium-doped air-clad optical fiber. IEEE Transactions on Nuclear Science, 2020, 67 (7), pp.1658-1662. 10.1109/TNS.2020.2972043 . hal-02902688

HAL Id: hal-02902688
https://hal.science/hal-02902688

Submitted on 16 Jul 2024

HAL is a multi-disciplinary open access archive for the deposit and dissemination of scientific research documents, whether they are published or not. The documents may come from teaching and research institutions in France or abroad, or from public or private research centers.

L'archive ouverte pluridisciplinaire **HAL**, est destinée au dépôt et à la diffusion de documents scientifiques de niveau recherche, publiés ou non, émanant des établissements d'enseignement et de recherche français ou étrangers, des laboratoires publics ou privés.

Remote Measurements of X-rays Dose Rate using a Cerium-doped Air-clad Optical Fiber

Jessica Bahout, Youcef Ouerdane, Hicham El Hamzaoui, Géraud Bouwmans, Mohamed Bouazaoui, Andy Cassez, Karen Baudelle, Rémi Habert, Adriana Morana, Aziz Boukenter, Sylvain Girard, Senior Member IEEE, and Bruno Capoen

***Abstract*—Cerium doped silica glasses are attractive materials for radiation dosimetry. In this work, Ce-doped air-clad optical fiber has been fabricated for real-time X-ray dose rate measurements through the radioluminescence (RL) signal. The structural properties of the obtained material were studied using Raman spectroscopy. The presence of Ce^{3+} ions inside the sol-gel-derived silica core was confirmed using photoluminescence (PL) measurements. This optical fiber, with a high numerical aperture, was tested as active and guiding material in an all-fibered remote X-ray dosimeter configuration. We demonstrated that the response dependence of RL versus dose rate is linear from 52 mGy(SiO_2)/s up to at least 1.5 Gy(SiO_2)/s, allowing to monitor the dose rate evolution during an irradiation run. The presented results confirm the potentialities of this microstructured optical fiber to monitor ionizing radiations in harsh environments. They also pave the way towards an alternative to the widely used approach that uses a scintillator material at the end of a transport optical fiber.**

***Index Terms*—Dosimetry, X-radiation, optical fiber, cerium, radioluminescence.**

I. Introduction

In the field of ionizing radiations dosimetry, optical fibers offer key advantages compared to conventional radiation sensors: small size, flexibility, intrinsic immunity to electro-magnetic interference and their ability for remote interrogation [1]-[3]. They can ensure the spatial separation of the radiation sensitive probe and the electronic processing system, which allows remote measurements in complex and narrow geometries of difficult-to-access and/or hazardous locations, without exposing the operator or the vulnerable electronics to the severe environment. Moreover, a real-time dosimeter device, with high spatial resolution, is also needed in the situations where there is a lack of charged particle equilibrium such as in ‘‘in vivo’’ dosimetry of small-size radiation fields [4]. Hence, based on optical fibers, real-time dosimeter devices, with high spatial resolution, can be envisaged. In the case of scintillation sensors, the system is based on material capable of converting ionizing radiation into detectable light. However, in this field, optical fibers, especially organic ones, were widely used only in passive configurations as guiding supports connected to optical transducers for the signal transport from the irradiation zone to the instrumentation one [5], [6]. Under UV or X-excitation, Ce^{3+}-doped silica glasses present visible luminescence peaking in the blue spectral domain [7], [8]. This emission with fast decay times is compatible with time-resolved dosimetry. It is also well matched to the spectral sensitivities of various optical photon detectors [9]. Based on this optical activity and under the condition to be able to tailor their shape and size, these cerium-activated glasses constitute promising scintillating materials. Recently, efficient cerium-doped silica glass was prepared, using the sol-gel route, for ionizing radiation dosimetry applications. In particular, glassy rods were drawn at high temperature to millimeter-sized canes. Thereafter, a small piece (10 mm-length) of this glass scintillator was connected to a transport inorganic passive optical fiber, allowing a remote monitoring of the X-ray dose rate through radioluminescence (RL) signal. The obtained results confirmed the potentialities of this material for real-time remote ionizing radiations dosimetry [10], [11]. In the approach of further reducing the sensing material size, and thus increasing its spatial resolution, an alternative to the use of a scintillator material at the end of an optical fiber could be the use of the fiber itself as both active and guiding materials. This is also of interest for distributed sensing along the length of the fiber. However, one of the main drawback effects of using optical fibers in high-energy radiation fields is the raise of light propagating attenuation through the fiber. The radiation-induced attenuation (RIA) effect has been extensively investigated, in different optical fibers, for radiation sensing applications [12], [13]. However, this RIA could be harmful for the transport of scintillating signal in the case of luminescence based sensors. This mostly concerns multicomponent glasses, which contain glass modifier elements that yield a decrease of the glass resistance to radiations [14]. On the other hand, pure silica glass is known for its radiation hardness, but it has almost

Manuscript received October 8, 2019. This operation was supported by Andra within the French government “Investissements d’Avenir” program: SURFIN Project. It was also partially supported by the ANR: LABEX CEMPI (ANR-11-LABX-0007) and the Equipex Flux (ANR-11-EQPX-0017), by The Ministry of Higher Education and Research, the Hauts-de-France Regional Council and the European Regional Development Fund (ERDF) through the Contrat de Projets Etat-Region (CPER Photonics for Society P4S).

J. Bahout, H. El Hamzaoui, B. Capoen, A. Cassez, K. Delplace, R. Habert, and M. Bouazaoui are with PhLAM Laboratory, Université de Lille, F-59000 Lille, France (e-mail: hicham.el-hamzaoui@univ-lille.fr).

Y. Ouerdane, A. Morana, A. Boukenter, and S. Girard are with Univ Lyon, Lab. Hubert Curien, CNRS UMR 5516, F-42000 Saint-Etienne, France.

no intrinsic scintillating property. Doping silica with Ce^{3+} ions presents advantages: (i) it provides efficient scintillating properties and (ii) reduces coloration due to the formation of radiation-induced colors centers [10], [15], [16]. Previous studies demonstrated the efficiency of Ce-doping to reduce the RIA in conventional optical fibers [2], [17]. Hence, to reduce its RIA, the use of an optical fiber as active/guide medium will require a core material with relatively high resistance to radiations and low overlap between the guided mode and the doped region in the core zone. Moreover, the fiber should have a high numerical aperture (NA), allowing a maximum amount of light emitted by the core doped zone to be captured and guided to a detector. For these reasons, an air-clad fiber design with a high NA and based on a pure silica host material, showing a high damage threshold, physical stability and strong chemical resistance [18]-[21], could be a promising solution. This air-clad geometry, with a Ce-doped core embedded in a secondary larger pure silica core, would have the advantage of limiting the re-absorption phenomena inside the doped core. Hence, in this paper, Ce-doped silica glass was prepared using the sol-gel method and was integrated as core material of an air-clad optical fiber. The RL response of this active material to X-ray exposure has been evaluated for the first time to our best knowledge. It constitutes our preliminary results of an effort undertaken to extend the use of active silica glasses to all-fibered remote ionizing radiation configurations.

II. Materials and Methods

A. Studied samples

Porous silica xerogel was synthetized, at PhLAM Laboratory of the University of Lille, using the sol-gel technique from tetraethylorthosilicate (TEOS) precursor as described elsewhere [22]. The obtained xerogel was stabilized at 1000°C and then soaked in an alcoholic solution containing cerium salts. Subsequently, the sample was withdrawn from the doping solution and dried at 50°C for 24 hours to remove solvent, while cerium dopant was retained within the nanopores. The doped matrix was then densified in helium atmosphere at 1200 °C for 2 hours. The air-clad fiber was fabricated at Fibertech Lille platform of the University of Lille using the stack-and-draw method. At first, a crack-free Ce-doped silica glass rod was drawn, under inert atmosphere, into a cane of millimeter size. This cane was sleeved with a pure silica tube and stacked with pure silica capillaries in an air-clad arrangement, aiming to improve the fiber attenuation by reducing its absorption. This has been managed by lowering the overlap between the guided mode and the doped region. The stack was then drawn into a final fiber form at high temperature (around 2000 °C).

The cross-section of the fiber was imaged using a Hitachi 3400N scanning electron microscope (SEM). The fiber structure consists of a central sol-gel silica core surrounded by a first silica clad, followed by a single ring of air holes as shown in the insets of Fig. 1. This fiber has an outer diameter of about 125 µm and a core diameter of about 90 µm. The sol-gel doped section has a diameter of about 20 µm. The air-clad fiber design was also chosen with silica thin webs of about 250 nm width, because of its high numerical aperture (NA), estimated to be about 0.6 at 500 nm, allowing a maximum amount of light emitted by the Ce^{3+} ions of sol-gel core to be captured and guided to a detector.

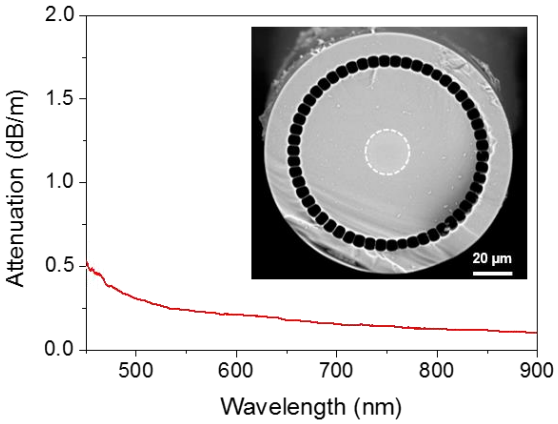

Fig. 1. Attenuation spectrum of cerium-doped air-clad optical fiber. Inset: SEM cross-section image of this fiber (the sol-gel doped zone has been schematized by a white dashed circle).

Background optical losses were measured by the cutback method using a supercontinuum source and an optical spectrum analyzer (OSA) to record the output spectrum (Fig. 1). The Ce-doped fiber presents an attenuation level with loss value of about 0.4 dB/m at 470 nm, corresponding to the wavelength of the maximum RL emission band of Ce^{3+} ions in host silica glass [11]. In the short wavelength region of this spectrum, an increase of the loss level can be observed. Although the used OSA did not enable attenuation measurements for wavelengths below 450 nm, this behavior could be related to the presence of the characteristic absorption bands of Ce^{3+} ions in the UV domain around 320 nm [10].

B. Raman measurements

The confocal micro-Raman spectra on the central sol-gel silica core and in the first silica clad were recorded using an Aramis (Jobin-Yvon) spectrometer. This setup is supplied by a CCD camera, a step motor, and 40× objective. A 633 nm He-Ne laser excitation was used. The spectra were acquired, at room temperature, with experimental conditions ensuring a spatial resolution of ~3 µm.

C. PL measurements

PL and time-resolved luminescence measurements were performed, at room temperature, using an optical parametric oscillator as excitation source. This former was equipped with a second harmonic generation nonlinear crystal pumped by the third harmonic of a Nd:YAG laser with pulse width of 5 ns and repetition rate of 10 Hz. For kinetics measurements, the light emitted by the samples was spectrally resolved by a grating with 300 grooves/mm and recorded by a gated intensified CCD equipped with a delay generator. PL spectra were collected by connecting the fiber to a QE pro spectrometer (Ocean optics).

D. RL experimental setup

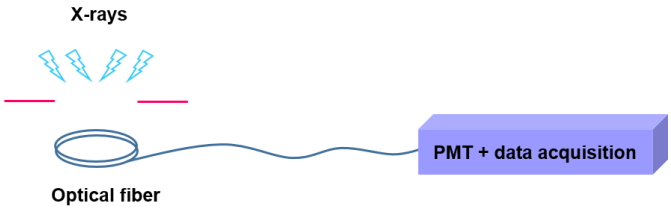

Fig. 2. Schematic illustration of the experimental setup used to characterize the RL response of the fiber material exposed to X-ray beam.

The external X-ray beam was delivered by the MOPERIX facility of Laboratoire Hubert Curien, operating at 100 kV and generating photons of ~ 40 keV average energy. The X-ray dose rate was driven by the electric current of the equipment. RL measurements were performed using 5 m-long Ce-doped air-clad fiber (Fig. 2). A 2 m-long piece of this fiber was winded on several circles, of about 16 cm in diameter and placed in a calibrated position of X-irradiator, ensuring uniform irradiation of all the fiber length. Under X-rays, the RL signal was then guided through the entire rest of the fiber towards a photomultiplier module (PMT, H9305-03 Hamamatsu). The acquisition was set with a numerical oscilloscope (Agilent Technologies InfiniiVision DSO7052B). The choice of exposing 2 m of the fiber length to X-rays has been made to enhance the exploitable RL signal in the investigated dose rate range.

III. EXPERIMENTAL RESULTS

A. Raman

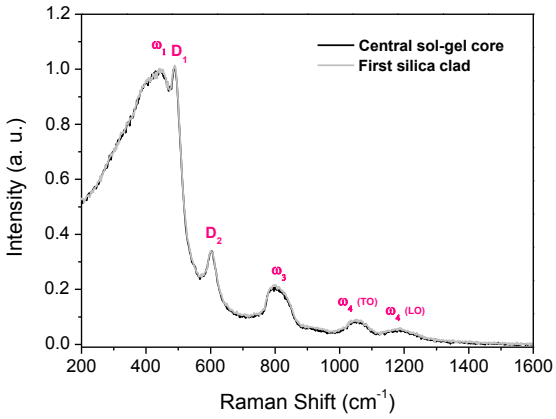

Fig. 3. Normalized Raman spectra of cerium-doped air-clad optical fiber recorded on the central sol-gel silica core and in the first silica clad.

Figure 3 presents the normalized Raman spectra of the cerium-doped air-clad optical fiber recorded on the central sol-gel silica core and in the first silica clad. They exhibit the well-known SiO_2 glass bands [23], including the large band centered around 440 cm^{-1} and attributed to the Si-O-Si network deformation vibration (ω_1). The two smaller bands at 490 cm^{-1} (D_1) and 603 cm^{-1} (D_2) are assigned to symmetric stretching modes of three- and four-member siloxane rings, respectively, in the silica network. The asymmetric band situated around 800 cm^{-1} (ω_3) is assigned to a complex vibration involving substantial silicon motion in addition to a bending movement of oxygen in a vitreous network. The high frequency bands (ω_4) at ~1050 and ~1200 cm^{-1} were attributed to a TO-LO pair splitting. It can be seen that independently on the position, the overall recorded Raman spectra are similar. This indicates no important structural variation between the doped sol-gel core and the first undoped silica cladding. Hence, the low doping level of cerium (about 300 ppm at.%) does not impact the structure of the host silica matrix.

B. Photoluminescence

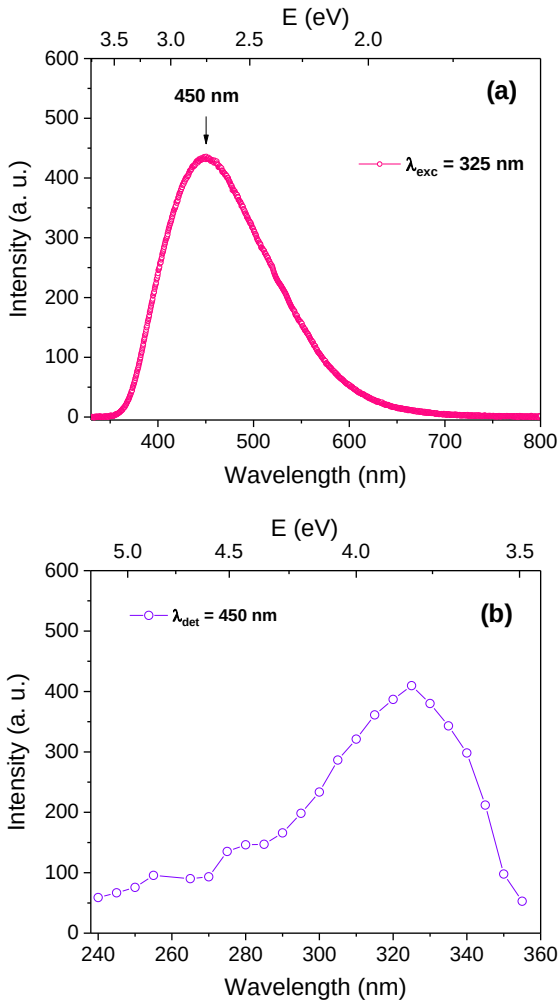

Fig. 4. (a) PL spectrum of cerium-doped air-clad optical fiber under 325 nm laser excitation. (b) Excitation spectrum at a detection wavelength of 450 nm of the same fiber.

PL spectrum of the cerium-doped air-clad optical fiber, under laser excitation at 325 nm, is presented in Fig. 4(a). It can be seen that the obtained spectrum exhibits broad band centered around 450 nm with a full width at half maximum (FWHM) of about 133 nm. This band is attributed, according to the literature [10], to the allowed 5d → 4f optical transition of Ce^{3+} ions. In Fig. 4(b) is reported the corresponding excitation spectrum, which consists of a broad band centered at about 325 nm, attributed to Ce^{3+} ions [10].

To further confirm that this blue PL corresponds to the emission by Ce^{3+} ions, we performed PL kinetics measurements under UV excitation.

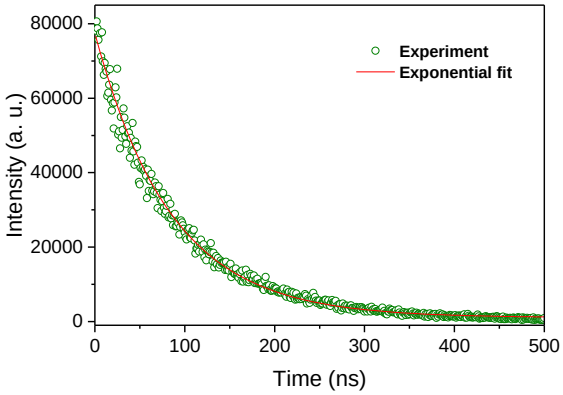

Fig. 5. PL decay curve recorded at 450 nm, under excitation at 322 nm and its corresponding mono-exponential curve fitting.

Fig. 5 shows the decay curve of the signal recorded at 450 nm upon excitation at 322 nm. PL kinetics show a mono-exponential behavior characterized by a decay time of about τ = 84 ns. This time, in the range of nanoseconds, is consistent with those reported for emitting Ce^{3+} ions dispersed in other silica-based glasses [24]-[26]. All these results confirm the presence of the active Ce^{3+} ions inside the core of our air-clad optical fiber.

C. Radioluminescence

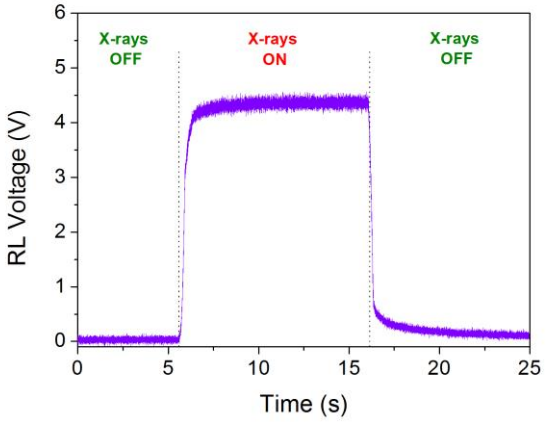

Fig. 6. RL signal under X-rays for a dose rate of 1.2 Gy(SiO_2)/s.

Fig. 6 shows the typical dynamics of the RL signal intensity collected by the PMT under a dose rate of 1.2 Gy(SiO_2)/s. As the X irradiation starts, the RL signal increases for a few seconds and tends toward a plateau. The mean voltage read on this plateau depends on the dose rate. The dose rate was evaluated with an ionization chamber, calibrated to provide dose rates in Gy(H_2O)/s. The measured values were then converted in Gy(SiO_2) by taking into account the ratio of mass attenuation coefficients between water and silica. The delayed response of the material to irradiation is due to carrier trap states. Indeed, during the irradiation, the prompt recombination causing the production of the RL signal is in competition with electron trapping by shallow and deep traps. However, as the electron traps are filled, the trapping probability decreases and then, more electrons become available for recombination. The RL signal rises to a steady-state level, which increases for each increasing dose rate.

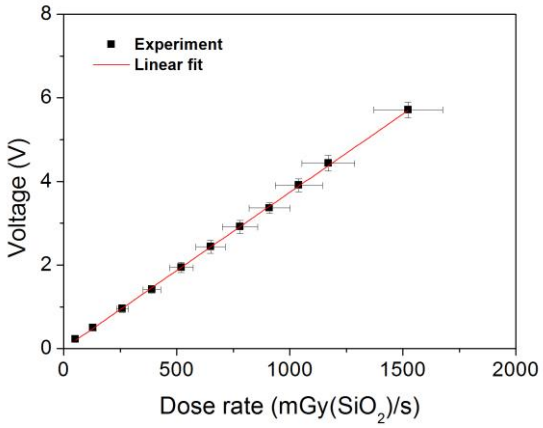

Fig. 7. Dose rate response of the Ce-doped air-clad optical fiber. The RL signal level was taken on the plateau.

Fig. 7 shows the evolution of the average RL signal, in the permanent regime (plateau), as a function of the X-ray dose rate. The dose rate dependence of the RL is clearly linear from 52 mGy(SiO_2)/s to at least 1.5 Gy(SiO_2)/s. It is to be stressed that, being given the response amplitude (Fig. 3), it should be possible to expose a much shorter fiber piece to ionizing radiation for the highest dose rate measurements. Moreover, further optimization of this air-clad fiber geometry by increasing the volume of the sol-gel doped zone is underway, which could be suitable for lower dose rate measurements with a reduced fiber length.

We performed a spectroscopic investigation to elucidate the mechanisms at the origin of the RL signal. The RL spectrum was recorded by connecting the fiber to a TM-UV/VIS mini-spectrometer (C10082CA Hamamatsu).

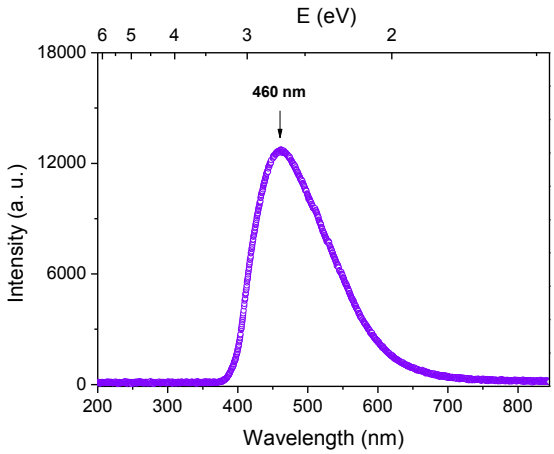

Fig. 8. Typical RL spectrum of cerium-doped air-clad optical fiber in the UV-visible range.

Fig. 8 presents a typical RL spectrum of cerium-doped air-clad optical fiber, in the whole UV-visible range. It shows RL emission band centered around 460 nm with a FWHM of about 130 nm. Moreover, no continuous background signal due to the stem effect has been observed [27]. Such stem effects are generally characterized by slowly varying signals against wavelength. The similarity of RL and PL [Fig. 3(a)] spectra

demonstrates that the RL process involves the same energy levels as the PL phenomenon: in both cases, the final transition occurs from 5d state to the split ground states 4f ($^2F_{5/2}$) and 4f ($^2F_{7/2}$) of trivalent Ce^{3+} ions [11]. The slight difference between PL and RL bands could be related to the different excitation-emission mechanisms in the PL and RL processes. Concerning the PL case, the Ce^{3+} ions are immediately excited by incident photon energy. On the other hand, in the RL, X-rays initially generate electron-hole pairs, which then relax through defect traps before the final radiative recombination on the excited centers.

IV. Conclusion

In this work, an air-clad Ce-doped optical fiber has been designed and fabricated to measure the RL signal under X-irradiation in an all-fibered configuration. Raman investigations indicated no important structural variations between the doped sol-gel core and the first undoped silica cladding. Photoluminescence measurements demonstrated the presence of trivalent active ions (Ce^{3+}) inside the sol-gel silica core of this fiber. Moreover, we have shown that the RL signal of such a component presents a linear behavior versus dose rate in a domain ranging from 52 to at least 1523 mGy(SiO_2)/s. Besides, RL process involves the same energy levels of Ce^{3+} ions as the PL phenomenon. Thanks to the obtained results, this doped optical fiber exhibits an interesting potential for ionizing radiation dosimetry applications. Besides, the high design flexibility of such air-clad fiber geometry can be adapted to use other silica glass-based efficient scintillator materials.

References

[1] S. O'Keeffe, C. Fitzpatrick, E. Lewis, and A.I. Al-Shamma'a, "A review of optical fibre radiation dosimeters," *Sensor Rev.*, vol. 28, no. 2, pp.136-142, 2008.

[2] S. Girard, A. Morana, A. Ladaci, T. Robin, L. Mescia, J.-J. Bonnefois, M. Boutillier, J. Mekki, A. Paveau, B. Cadier, E. Marin, Y. Ouerdane, and A. Boukenter, "Recent advances in radiation-hardened fiber-based technologies for space applications," *J. Opt.*, vol. 20, no. 9, pp. 093001-1–093001-48, Aug. 2018.

[3] S. Delepine-Lesoille, S. Girard, M. Landolt, J. Bertrand, I. Planes, A. Boukenter, E. Marin, G. Humbert, S. Leparmentier, J.-L. Auguste, and Y Ouerdane, "France's State of the Art Distributed Optical Fibre Sensors Qualified for the Monitoring of the French Underground Repository for High Level and Intermediate Level Long Lived Radioactive Wastes," *Sensors* vol. 17, 1377, Jun. 2017.

[4] I. J. Das, G. X. Ding, and A. Ahnesjö, "Small fields: nonequilibrium radiation dosimetry," *Med. Phys.*, vol. 35, no. 1, pp. 206-215, Jau. 2008.

[5] Y. Hu, Z. Qin, Y. Ma, W. Zhao, W. Sun, D. Zhang, Z. Chen, B. Wang, H. Tian, and E. Lewis, "Characterization of fiber radiation dosimeters with different embedded scintillator materials for radiotherapy applications," *Sens. Actuators A Phys.*, vol. 269, pp. 188-195, Jan. 2018.

[6] S. Buranurak and C.E. Andersen, "Fiber-coupled Al_2O_3:C radioluminescence dosimetry for total body irradiations," *Radiation Measurements*, vol. 93, pp. 46-54, Oct. 2016.

[7] C. Canevali, M. Mattoni, F. Morazzoni, R. Scotti, M. Casu, A. Musinu, R. Krsmanovic, S. Polizzi, A. Speghini, and M. Bettinelli, "Stability of luminescent trivalent cerium in silica host glasses modified by boron and phosphorus," *J. Amer. Chem. Soc.*, vol. 127, no. 42, pp. 14681-14691, Oct. 2005.

[8] A. Vedda, N. Chiodini, D. Di Martino, M. Fasoli, S. Keffer, A. Lauria, M. Martini, F. Moretti, G. Spinolo, M. Nikl, N. Solovieva, and G. Brambilla, "Ce^{3+}-doped fibers for remote radiation dosimetry," *Appl. Phys. Lett.*, vol. 85, no. 26, p. 6356, Dec. 2004.

[9] I. G. Valais, S. David, C. Michail, C. Nomicos, G. Panayiotakis, I. Kandarakis "Comparative evaluation of single crystal scintillators under X-ray imaging conditions," *J. Instrum.*, vol. 4, no. 6, pp. P06013, Jun. 2009.

[10] H. El Hamzaoui, B. Capoen, N. Al Helou, G. Bouwmans, Y. Ouerdane, A. Boukenter, S. Girard, C. Marcandella, O. Duhamel, G. Chadeyron, R. Mahiou and M. Bouazaoui, "Cerium-activated sol-gel silica glasses for radiation dosimetry in harsh environment," Mater. Res. Exp., vol. 3, no. 4, pp. 046201-1–046201-7, Apr. 2016.

[11] N. Al Helou, H. El Hamzaoui, B. Capoen, G. Bouwmans, A. Cassez, Y. Ouerdane, A. Boukenter, S. Girard, G. Chadeyron, R. Mahiou, and M. Bouazaoui, "Radioluminescence and Optically Stimulated Luminescence Responses of a Cerium-Doped Sol-Gel Silica Glass Under X-Ray Beam Irradiation," *IEEE Trans. Nucl. Sci.*, vol. 65, no. 8, pp. 1591-1597, Aug. 2018.

[12] S. Girard, J. Kuhnhenn, A. Gusarov, B. Brichard, M. Van Uffelen, Y. Ouerdane, A. Boukenter, and C. Marcandella, "Radiation effects on silica-based optical fibers: recent advances and future challenges," *IEEE Trans. Nucl. Sci.*, vol. 60, no. 3, pp. 2015-2036, Jun. 2013.

[13] A. V. Faustov, A. Gusarov, M. Wuilpart, A. A. Fotiadi, L. B. Liokumovich, I. O. Zolotovskiy, A. L. Tomashuk, T. de Schoutheete, and P. Megret, "Comparison of gamma-radiation induced attenuation in Al-doped, P-doped and Ge-doped fibres for dosimetry," IEEE Trans. Nucl. Sci., vol. 60, no. 4, pp. 2511-2517, Aug. 2013.

[14] E. J. Friebele, "Radiation Effects in Optical Properties of Glass," Edited by D.R. Uhlmann and N.J. Kreidl. The American Ceramic Society, Westerville, OH, USA, 205-262 (1991).

[15] J. S. Stroud, "Color-Center Kinetics in Cerium-Containing Glass," *J. Chem. Phys.* vol. 43, pp. 2442-2450, Oct. 1965.

[16] J. S. Stroud, "Color Centers in a Cerium-Containing Silicate Glass," *J. Chem. Phys.* vol. 37, pp. 836-841, Aug. 1962.

[17] S. Girard, M. Vivona, A. Laurent, B. Cadier, C. Marcandella, T. Robin, E. Pinsard, A. Boukenter, and Y. Ouerdane, "Radiation hardening techniques for Er/Yb doped optical fibers and amplifiers for space application," *Opt. Express* vol. 20, no. 8, pp. 8457-8465, Apr. 2012.

[18] N. P. Bansal and R. H. Doremus, Handbook of Glass Properties. New York: Academic Press (1986).

[19] B. Brichard, P. Borgermans, A. F. Fernandez, K. Lammens, and M. Decreton, "Radiation Effect in Silica Optical Fiber Exposed to Intense Mixed Neutron-Gamma Radiation Field," *IEEE Trans. Nucl. Sci.* vol. 48, no. 6, pp. 2069-2073, Dec. 2001.

[20] O. M. Efimov, K. Gabel, S. V. Garnov, L. B. Glebov, S. Grantham, M. Richardson, and M. J. Soileau, "Color-center generation in silicate glasses exposed to infrared femtosecond pulses," *J. Opt. Soc. Am. B* vol. 15, no. 1, pp. 193-199, Jau. 1998.

[21] B. H. Babu, N. Ollier, M. L. Pichel, H. El Hamzaoui, B. Poumellec, L. Bigot, I. Savelii, M. Bouazaoui, A. Ibarra, and M. Lancry, "Radiation hardening in sol-gel derived Er^{3+}-doped silica glasses," *J. App. Phys.* vol. 118, no. 12, pp. 123107-1–123107-7, Sep. 2015.

[22] H. El Hamzaoui, L. Courthéoux, V. Nguyen, E. Berrier, A. Favre, L. Bigot, M. Bouazaoui, and B. Capoen, "From porous silica xerogels to bulk optical glasses: The control of densification," *Mater. Chem. Phys.* vol. 121, nos. 1-2, pp. 83-88, May 2010.

[23] H. El Hamzaoui, M. Bouazaoui, and B. Capoen, Raman investigation of germanium- and phosphorus-doping effects on the structure of sol–gel silica-based optical fiber preforms, *J. Mol. Struct.* vol. 1099, pp. 77-82, Nov. 2015.

[24] Y. Ishii, K. Arai, H. Namikawa, M. Tanaka, A. Negishi, and T. Handa, "Preparation of Cerium- Activated Silica Glasses: Phosphorus and Aluminum Codoping Effects on Absorption and Fluorescence Properties," *J. Am. Ceram. Soc.*, vol. 70, no. 2, 72-77, Feb. 1987.

[25] W. Chewpraditkul, Y. Shen, D. Chen, B. Yu, P. Prusa, M. Nikl, A. Beitlerova, and C. Wanarak, "Luminescence and scintillation of Ce^{3+}-doped high silica glass," *Opt. Mater.*, vol. 34, no. 11, 1762-1766, Sep. 2012.

[26] G. Okada, S. Kasap, and T. Yanagida, "Optically- and thermally-stimulated luminescences of Ce-doped SiO_2 glasses prepared by spark plasma sintering," *Opt. Mater.*, vol. 61, 15-20, Nov. 2016.

[27] N. Chiodini, A. Vedda, and I. Veronese, "Rare Earth Doped Silica Optical Fibre Sensors for Dosimetry in Medical and Technical Applications," *Adv. Opt.* 974584 (9 pp), Oct. 2014.